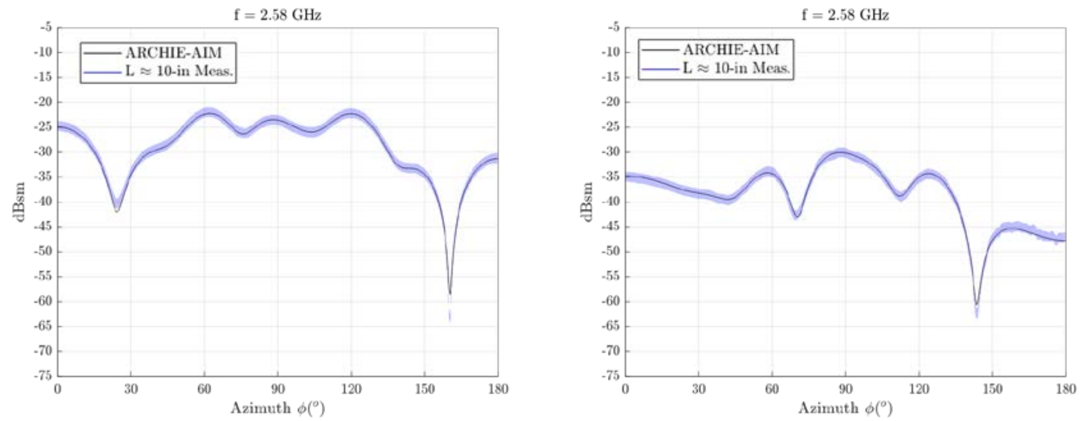

Figure 1: The HH ($\sigma_{\phi\phi,\mathrm{dB}}$, left) and VV ($\sigma_{\theta\theta,\mathrm{dB}}$, right) polarized RCS for the solid resin almond of length L= 9.936 in at frequency f = 2.58 GHz.

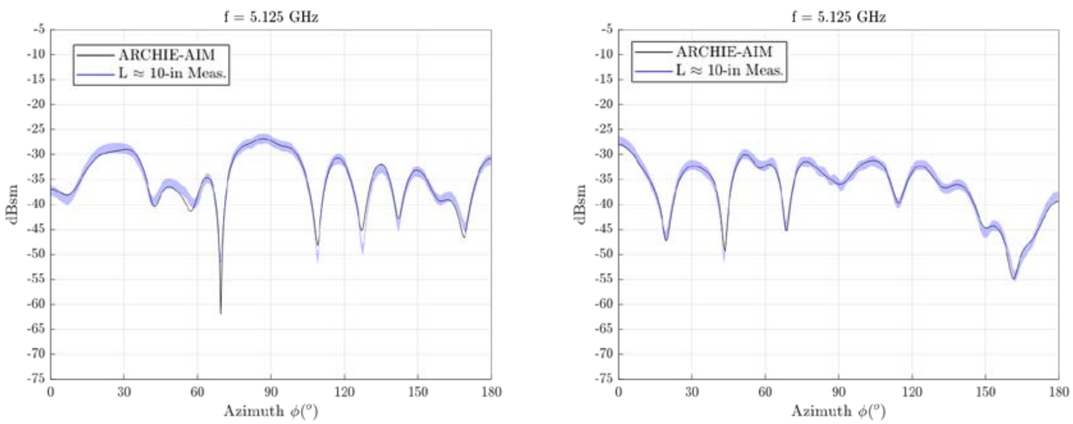

Figure 2: The HH ($\sigma_{\phi\phi,\mathrm{dB}}$, left) and VV ($\sigma_{\theta\theta,\mathrm{dB}}$, right) polarized RCS for the solid resin almond of length L= 9.936 in at frequency f = 5.125 GHz.

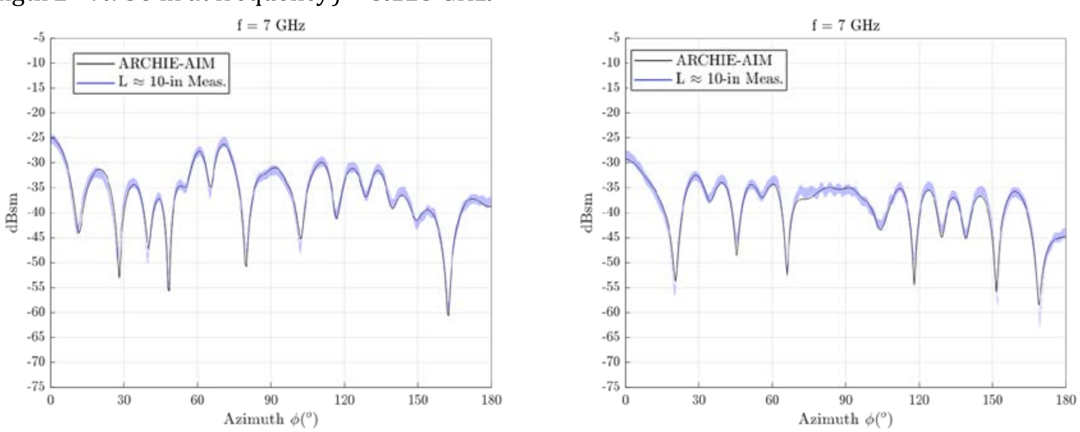

Figure 3: The HH ($\sigma_{\phi\phi,\mathrm{dB}}$, left) and VV ($\sigma_{\theta\theta,\mathrm{dB}}$, right) polarized RCS for the solid resin almond of length L= 9.936 in at frequency f = 7 GHz.

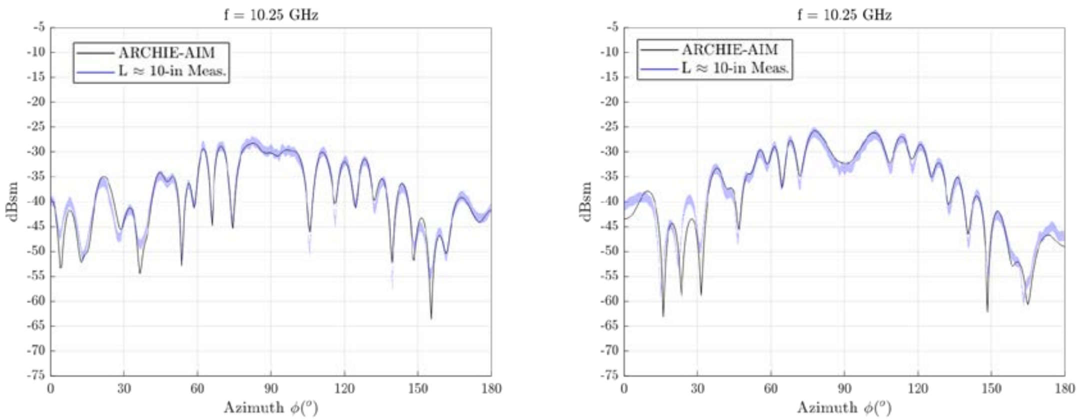

Figure 4: The HH ($\sigma_{\phi\phi,\mathrm{dB}}$, left) and VV ($\sigma_{\theta\theta,\mathrm{dB}}$, right) polarized RCS for the solid resin almond of length L= 9.936 in at frequency f = 10.25 GHz.

The above RCS results are that of the reference measurement and simulation data in the benchmark suite. The measurement data in the suite are the same as that shown in [1] and are plotted within a ∓ 1 dB window to represent the measurement uncertainties. The simulation data are slightly different than that shown in [1] due to the change in the Debye model parameters (see the "problem description" document and [2] for the reason behind this change).

Notes

1. The measurement and simulation data are provided at every 0.5^{o} in the azimuthal range.
2. The simulation data were calculated by using the ARCHIE-AIM code, a frequency-domain FFT-accelerated integral-equation solver developed at UT Austin [3]-[5], and are the same as the finest mesh (≈0.6-mm average edge length) results in [1],[6].

References

[1] J. T. Kelley, A. E. Yilmaz, D. A. Chamulak, and C. C. Courtney, "Measurements of non-metallic targets for the Austin RCS benchmark suite," in *Proc. Ant. Meas. Tech. Assoc. (AMTA) Symp.*, Oct. 2019.

[2] J. T. Kelley, D. A. Chamulak, C. C. Courtney, and A. E. Yilmaz, "Measurements of non-metallic targets for the Austin RCS benchmark suite," *presentation in AMTA Symp.,* Oct. 2019. Available: https://github.com/UTAustinCEMGroup/AustinCEMBenchmarks/Austin-RCS-Benchmarks/AMTA2019presentation.pdf

[3] M. F. Wu, G. Kaur, and A. E. Yılmaz, "A multiple-grid adaptive integral method for multi region problems," *IEEE Trans. Antennas Propag.*, vol. 58, no. 5, pp. 1601-1613, May 2010.

[4] F. Wei and A. E. Yılmaz, "A more scalable and efficient parallelization of the adaptive integral method part I: algorithm," *IEEE Trans. Antennas Propag.*, vol. 62, no.2, pp. 714-726, Feb. 2014.

[5] J. W. Massey, V. Subramanian, C. Liu, and A. E. Yılmaz, "Analyzing UHF band antennas near humans with a fast integral-equation method," in *Proc. EUCAP*, Apr. 2016.

[6] J. T. Kelley, D. A. Chamulak, C. C. Courtney, and A. E. Yilmaz, "Rye Canyon radar cross-section measurements of benchmark almond targets," *IEEE Ant. Popag. Soc. Mag.*, Feb. 2020.